TOTAL SUSPENDED SOLIDS AND FLOW REGIME EFFECTS ON PERIPHYTON DEVELOPMENT IN A LABORATORY CHANNEL

C. Birkett, E. W. Tollner, D. K. Gattie

ABSTRACT. *Flow regime and total suspended solids (TSS), along with chemical and biological parameters associated with urbanization and intensive agriculture/aquaculture, impact benthic organisms, which represents the food chain foundation in aquatic systems. We designed this experiment to begin the integration of physical flow regime effects along with chemical and biological indicators on periphyton, an important benthic organism indicator, towards a goal of using periphyton (live biomass containing chlorophyll a) and pheophytin (dead chlorophyll−containing biomass) in assessments of stream health. Physical flow regimes in a laboratory flume were created using multiple roughness conditions and an in−channel weir. Results suggested that one could model the hydraulic regime with a hydraulic model, HEC−RAS, to within 2% to 11% of measured velocity values. Thus, one may roughly but not precisely move computed velocities from the flume to the field. Significant interactions between biological response and hydraulic and TSS factors were observed, and the study suggested several indicators of periphyton−pheophytin response that are potentially relevant to ecological engineering applications featuring a channel. Increased mean velocities significantly reduced ($P < 0.05$) live periphyton and filament length. The 200 mg L^{-1} TSS level significantly reduced ($P < 0.05$) biomass and filament development. The effect of TSS was least where velocity was highest and depth was most shallow, which had the least effect on light absorption and resulted in the least sediment deposition. The intermediate TSS level (100 mg L^{-1}) appeared to stimulate a growth response based on periphyton and filament length, although the effect was less noticeable where velocities were higher. Pheophytin tended to be highest in conditions resulting in lower periphyton values, consistent with the notion that regimes imparting physical stress would harbor the highest concentration of pheophytin. The periphyton/filament length ratio tended to be lowest in velocities less than 0.75 m s^{-1} except in the high TSS case, where both periphyton and filament length were low. Low velocities and low to moderate TSS would provide the most biomass for grazing organisms and would result in the most effective nutrient filtering due to long filament length. High periphyton/pheophytin ratios were associated with high TSS, velocities exceeding ~0.5 m s^{-1}, or both. Sloughing could occur in systems with a pulsing velocity where the pulse period was long enough for growth to occur in the quiescent interval.*

Keywords. *Biomass, Chlorophyll a, Pheophytin, Suspended sediment, Turbulence.*

Societies are beginning to appreciate the value of restoration and conservation (Bockelmann et al., 2004) because pragmatic stormwater management and aquacultural production system benefits are often synergistic with the abundance and diversity of biota associated with stream biological integrity (Hill et al., 2003). An understanding of the underlying science principles operating at stream boundaries is essential to realize how human and other biotic activity can be mutually benefited. More importantly, benthics represented a temporally integrated assessment of stream integrity. However, there are few design guidelines relating to how one may maximize the use of benthics for biomass production or for nutrient removal.

One of the many benthic organisms affected by human activities is periphyton. Periphyton is used as a biological indicator to examine the quality and pollution of surface waters (Sansone et al., 1998). Periphyton has a naturally high number of species and is an important source of food for many of the higher−level organisms in the stream (Sabater et al., 2000). Periphyton also plays a major role in the metabolic conversion and partial removal of biodegradable material in wetlands, rivers, and streams (Vyzamal, 1988; Saravia et al., 1998) and aquacultural systems. Periphyton biomass is affected by many biotic and abiotic factors. Harding et al. (1999) indicated that agricultural intensity and physical conditions associated with agriculture activity (e.g., impacted waters, high TSS and temperature) were strongly associated with the composition of benthic assemblages. Periphyton is beginning to receive appreciation as a fundamental component in many aquaculture production systems, waste treatment systems, and storm water management systems.

There is considerable information in the literature concerning effects of various pollution constituents and light interactions on periphyton growth (e.g., Rosemond, 1993; Rosemond et al., 1993; Rosemond et al. 2001). Wastewater discharge carries large amounts of nutrients that can lead to

Submitted for review in March 2006 as manuscript number BE 6432; approved for publication by the Biological Engineering Division of ASABE in February 2007.

The authors are **Clayton Birkett,** Engineering Technician, USDA National Center for Cool and Cold Water Aquaculture, Kearneysville, West Virginia; **Ernest Tollner, ASABE Member Engineer,** Professor, and **David K. Gattie, ASABE Member Engineer,** Assistant Professor, Department of Biological and Agricultural Engineering Department, University of Georgia, Athens, Georgia. **Corresponding author:** Ernest W. Tollner, Department of Biological and Agricultural Engineering, Driftmier Engineering Center, University of Georgia, Athens, GA 30602; phone: 706−542−3047; fax: 706−542−8806; e−mail: btollner@engr.uga.edu.

  ISSN 0001−2351

large algal assemblages, resulting in subsequent eutrophication (Bokn et al., 2002; Mattila and Raisanen, 1998; Boynton et al., 1995; Pringle and Yamasaki, 1997; Riegman et al., 2002). Procedures for culturing and measuring periphyton and procedures for measuring pheophytin are well described in references cited previously. These procedures are based on assessing periphyton and pheophytin using spectrometric approaches enabling assessment of chlorophyll *a* (indicative of periphyton live biomass) and pheophytin (indicative of periphyton dead/senescent biomass) concentrations. This study is designed to focus more on physical factors affecting periphyton development, where much less research has been reported.

Studies have shown that turbulence and velocity have important effects on periphyton biomass (Bergstedt et al., 2004; Quinn et al., 1996; Nikora et al., 1997). Shear velocity and turbulence are factors in the effect of tractive force on the bottom of a stream system. Tractive force, the force exerted by flowing water, can be a factor in the attachment processes of periphyton by making the habitat unsuitable and by physically removing the periphyton from the attached substrate (Asaeda and Hong Son, 2000; Lau and Liu, 1993). Flumes are used as micro/mesocosm environments for studies of physical effects (e.g., Hondzo and Wang, 2002) and transport phenomena (e.g., Cokgor and Kucukali, 2004) associated with ecological systems.

Increased exposure to turbulence increases the sloughing of epiphytic organisms from surfaces (Eriksson and Weisner, 1996). In addition to affecting growth, fluid velocity also affects the height to which the periphyton can grow (Nikora et al., 1997). Saravia et al. (1998) examined the degree of sloughing in periphyton. The degree of sloughing was greater in low−velocity sites, meaning that changes in current velocity had a greater influence at these sites than in the rapid current sites. In addition, velocity was inversely related to attached biomass.

The theoretical detachment curve of Hondzo and Wang (2002) shows periphyton persistence as a function of the nondimensional critical shear stress and decreasing L/d ratios, where L/d is the ratio of filament length to filament diameter. It was determined that algal removal increases as shear rate increases. These studies suggest that one should account for the effects of periphyton at the boundary of systems involving open or closed conduit hydraulic processes. The Hondzo and Wang (2002) detachment curves do not account for TSS and are oriented toward micromorphology rather than macroscopic filament length. Nikora et al. (2002) stated that knowledge of mass transfer processes and physical interactions between periphyton and the turbulent stream flow, which control periphyton growth and losses, may become critical to understanding the function of natural benthic communities in streams.

In our view, the Hondzo and Wang (2002) study showed that one could use a recirculating flume as a microcosm to study hydraulic factors affecting periphyton development. The studies themselves are not readily scaled to a field environment as they stand. Models such as HEC−RAS enable one to evaluate not only mean velocity, but also other parameters related to forces on flow boundaries, such as tractive force and shear velocity. Thus, knowledge of tractive force and shear velocity in the laboratory could be readily taken to the field with HEC−RAS analyses. HEC−RAS is a one−dimensional steady and unsteady flow model capable of handling mixed subcritical and supercritical flows (Brunner, 2002).

Ecological ramifications of TSS loads have been observed, including destruction of habitat, decreased fecundity, and inhibited feeding (Parkhill and Gulliver, 2002). Elevated TSS levels can negatively affect fish, aquatic insects, other invertebrates, and algae (Schofield et al., 2004). Eroded silts and clays seriously reduce light penetration in some streams (Hill, 1996). Filamentous algal assemblages effectively serve as filters with the net effect of removing suspended particulate materials from the water column (Vyzamal, 1988; Stevenson, 1996), hence the significance of filament length along with biomass. We envision that flow regime guidelines for systems including periphyton can be established that will lead to adequately engineered and ecologically sustainable aquatic systems for a variety of purposes such as stormwater management, nutrient abatement, or aquacultural systems. This study is a tentative first step towards that end.

Objectives

The overall objective of this study was to build and test a concept for a periphyton study microcosm wherein interactions among hydraulic regime, physical factors, and potential chemical factors on periphyton growth could be studied. This study focused on hydraulic regime and TSS. The laboratory flume experiments focused on three specific objectives: (1) to determine the efficacy of using a hydraulic simulation model, HEC−RAS, to anticipate flows in field channels with a widely varying hydraulic regime over the channel length, and (2) to test interaction between selected flow parameters and total suspended solids (TSS) on selected periphyton biomass and filament length indicators.

Materials and Methods

The experiments were performed using a hydraulic demonstration flume (model B−16, Engineering Laboratory Design, Inc., Lake City, Minn.). The flume is 3 × 0.30 × 0.30 m and equipped with two pumps, a collection tank, and precalibrated orifice flowmeters.

The flume was divided into two identical 0.15 × 3 m channels, with each channel serving as a replication. A 0.30 m length of 25.4 mm gravel was placed 0.30 m from the entrance of the flume to dissipate entrance energy. It provided an additional flow regime or location. A broad crested weir (crest length of approx. 100 mm and crest width the same as the 0.15 m waterway width) was formed approximately 1 m from the discharge end. There were 42 test tiles (21 in each channel): one placed on the rocks (subcritical flow), eight placed downslope from the weir (supercritical), four on top of the weir (critical flow), and eight placed upslope from the weir (additional subcritical flow). The setup is shown in figure 1. A flow rate of approximately 0.005 $m^3 s^{-1}$, evenly divided between the two channels, was maintained throughout the study.

An constant−temperature anemometer (model IFA−300, TSI, Inc., Shoreview, Minn.) equipped with a one−dimensional probe was used to measure the mean velocity and turbulent (RMS) velocity at each testing site with five measurements per site, and values were averaged at each site in each of the two channels. Isotropic turbulence was assumed. Anemometers have been used to measure flow rate

Figure 1. Laboratory flume setup showing the rock bottom and tiled zone upstream from the weir and the tiled zone below the weir.

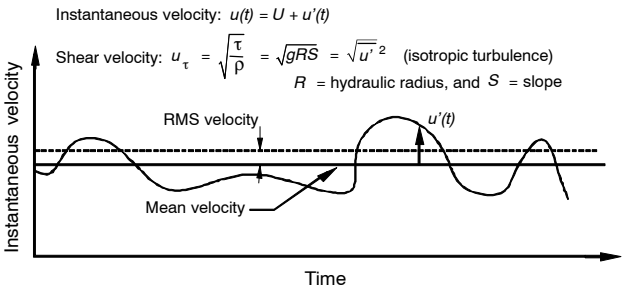

Figure 2. Key turbulence parameters and relationships for a hypothetical steady, isotropic turbulent flow, where isotropic implies an RMS velocity that is invariant with orientation.

and turbulence parameters in various studies (e.g., Nezu et al., 1997; Tollner et al., 2005). The turbulent parameters of interest are shown in figure 2. The mean and isotropic RMS velocity was measured in this study.

Once the anemometer was calibrated, the flume was started, and mean velocity and turbulent (RMS) velocity measurements were made at designated locations on the rocks, upslope tile, weir, and downslope tile. Mean and RMS velocities were measured at 0.6 × water depth to enable mean velocity comparisons with the results of a flume model using HEC–RAS (version 3.1.2). HEC–RAS uses the implicit method in solving the gradually varied flow equation. Boundary conditions were the measured flow depth at the inlet and outlet.

Manning n values were initially assigned as 0.009 for the acrylic flume itself, 0.013 for the divided acrylic, 0.018 for the tiles, and 0.028 for the gravel, based on tabulated values and ranges given by Chow (1959) and for the 25 mm angular rock, based on size correlations given by Simons and Senturk (1992). Inlet (0.045 ±0.001 m) and outlet (0.0165 ±0.001 m) water elevations were established using a hook gauge. The bottom height and roughness condition of the channel were evaluated within published extremes to best model the change in height from the rocks to the tiles to the bottom of the flume. A velocity comparison between the anemometer and the HEC–RAS model was made to determine the viability of the computer model. The HEC–RAS–reported velocity was the computed average velocity along the flume.

Stigeoclonium tenue, important in the southeastern U.S., was selected to represent periphyton in this study. Thirty milliliters of *Stigeoclonium tenue* (Kutz), obtained from the Culture Collection of Algae at the University of Texas at Austin, provided the innoculum for this study.

The periphyton was grown on prepared 75 × 75 mm white ceramic tiles for three weeks in an incubator. The incubator was configured with 20°C and a light/dark cycle of 13/11 h. The ceramic tiles were used to facilitate periphyton photosynthesis measurements. The inoculated tiles were placed in four 305 × 152 × 51 mm glass baking dishes, 12 test tiles per dish, in an incubator for initial growth in standard freshwater Wright–Chu (WC) medium (Guillard and Lorenzen, 1972). The testing tiles were scraped every two to three days to simulate grazing. The periphyton tiles were then moved into the test flume, which was located in a closed room with growth lights controlled to simulate incubator conditions. The light level of the commercially available growth lights on the flume was approximately 10% of light expected in clear–sky conditions (Birkett, 2005). The 10% light level approximated the light level seen in shaded waterways at similar TSS levels. Immediately after transfer of the tiles to the flume and flow initiation, much biomass sloughed off over the entire flume due to the water velocity in the various locations along the flume. This sloughing removed loose algal biomass and allowed for growth of new flow–tolerant biomass.

Testing cycles ran 20 days. Deionized water and the WC medium were used in the flume and were changed every five days. After each 20–day cycle, the flume was drained and wiped with a cloth to remove the periphyton that had grown on the side of the flume. Algal tiles were allowed to sit in standing water so that the filaments were fully extended, thereby enabling filament length measurement. Filament lengths were measured randomly at three locations (upper, weir, and lower sections with four measurements per section from both channels) and averaged. Tiles were then transferred from the flume and analyzed four times per test location (channels 1 and 2 composited) to determine chlorophyll *a* and pheophytin using the procedure of Steinman and Lamberti (1996). This procedure was repeated at each TSS level. The concentration of chlorophyll *a* indicated periphyton live cells, while the pheophytin concentration indicated periphyton dead/senescent cells.

Reagent–grade kaolin (Aldrich Chemical Co., Milwaukee, Wisc.) served as the TSS source for the runs containing sediment. Colloidal kaolin was chosen to minimize damage to the recirculation pumps. TSS levels were set at 0 mg L^{-1} (control), 100 mg L^{-1}, and 200 mg L^{-1}. A TSS threshold of 284 mg L^{-1} has been reported as the upper limit for periphyton growth (USEPA, 2001).

Selected water quality tests (pH, conductivity, BOD, total N, total P, ortho–PO_4, ammonia, and nitrate/nitrite ratio) were run at the beginning and end of each testing cycle, at each TSS level, to document any significant water quality changes. Based on water quality measurements, ammonia and pH remained constant over the entire experiment. All other nutrient readings trended upward as TSS level increased, although changes were not significant ($P \geq 0.05$). Birkett (2005) provides additional details.

The periphyton growth experiment was replicated twice at each TSS level. All results were analyzed using a general linear ANOVA, completely random design procedure or the Student–Newman–Keuls (SNK) multiple comparison

procedure, as appropriate, in the NCSS statistical software package (Hintze, 2004).

Results and Discussion

Flow Regime Definition and Modeling

Efforts were made to adjust the Manning n values within published ranges for the acrylic flume, tiles, and rock materials, with the flume schematically configured as shown in figure 3. Flow regime and location data are summarized in table 1. HEC–RAS–modeled velocities of the flow locations were within 5% of the measured velocities once the final adjustments were made to the Manning n values as shown in table 1. The mean velocities in channels 1 and 2 showed no significant difference in the upper and lower locations, but they did show a significant difference in the rock section ($P \leq 5\%$), which we attributed to slight differences between the rock structures in that section. Measurements from the two channels were then combined.

HEC–RAS depth was compared to the actual flume depth measured by a hook gauge. The HEC–RAS depth was 0.025 to 0.026 m higher (e.g., about half the thickness of the rock layer) than actual mean depth measured by hook gauge in the region from the weir toward the flume inlet, suggesting that some flow was occurring through the media. Observed versus predicted depth was within 9 mm below the weir, with HEC–RAS–predicted depth being slightly larger. This systematic error was attributed to:

- The possibility that HEC–RAS tends to slightly overpredict water profile elevations (refer to www.haestad.com for a forum on the performance of HEC–RAS, where the systematic overprediction of water surface elevation is discussed).
- Boundary layer effects are never able to fully manifest due to the short flow regime distances.
- Two–dimensional effects due to channel narrowness that HEC–RAS was unable to model.

It was interesting to note that the periphyton development over time in each testing cycle had little effect on the flow depth, suggesting that the effect on effective channel roughness was very small.

RMS velocity measurements were made with the anemometer along the channel centers. Shear velocity was computed from depth, slope, and fluid density. Shear velocity tracks the RMS velocity in all regions except the upstream test region above the weir, suggesting the possibility that the assumption of isotropic turbulence may not apply in this zone. The Froude number calculation indicates supercritical flow below the weir and subcritical flow above the weir, with critical flow at the weir, as one would expect. Chow (1959) provided definitions and formulas for computing Froude number, tractive force, and shear velocity.

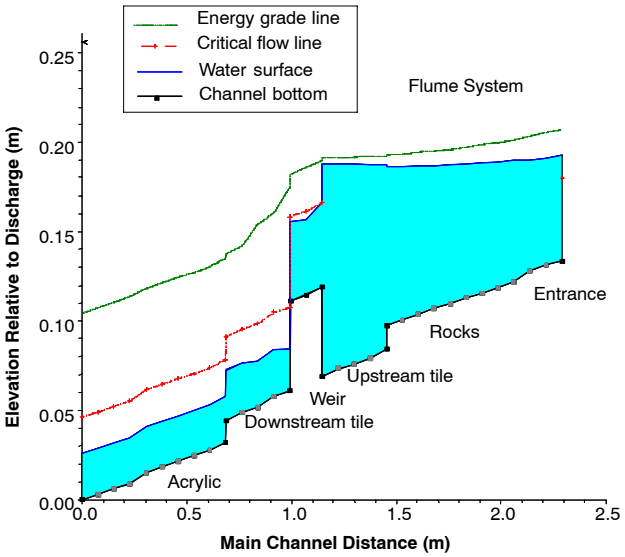

Figure 3. Typical channel flow profile showing HEC–RAS–modeled water depth, critical flow depth, energy grade line, and major channel features.

Based on comparison of HEC–RAS mean velocities and Froude number results with anemometer mean velocities, we suggest that small flumes are useful as periphyton microcosms and that HEC–RAS can be used to accurately model and scale these systems to some (predominantly one–dimensional) field systems in spite of the systematic overprediction of depth.

Table 2 shows additional results and comparison of the anemometer and HEC–RAS velocity values wherein HEC–RAS was further tuned by varying the Manning n (within published variations for the particular roughness condition) for the respective regions. The HEC–RAS mean velocity values were −3% to 4% different from the anemometer mean velocity values. In the rock section, the difference was 11%, representing the worst–case scenario. The errors were some–

Table 1. Selected velocity and flow regime characterization as a function of position in the flume.

	Mean ±Standard Error of Mean Statistics[a]			
Feature or Measurement	Rocks	Upstream Tile	Weir	Downstream Tile
Distance from discharge (m)	1.57	1.23	1.00	0.77
Mean velocity (m s^{-1})	0.49 ±0.003	0.30 ±0.001	0.75 ±0.001	1.18 ±0.007
HEC–RAS velocity (m s^{-1})[b]	0.42 ±0.004	0.31 ±0.003	0.78 ±0.01	1.21 ±0.025
Measured depth (m)	0.042 ±0.005	0.079 ±0.003	0.021 ±0.001	0.013 ±0.001
HEC–RAS depth (m)[b]	0.067 ±0.002	0.105 ±0.001	0.040 ±0.001	0.022 ±0.001
Change in depth (m)[c]	0.025	0.026	0.019	0.009
RMS velocity (m s^{-1})	0.085 ±0.044	0.118 ±0.004	0.079 ±0.051	0.160 ±0.016
Shear velocity (m s^{-1})	0.066 ±0.015	0.027 ±0.002	0.074 ±0.002	0.134 ±0.010
Froude number	0.52 ±0.16	0.27 ±0.19	1.09 ±0.25	2.39 ±0.35

[a] Statistics are shown with ±1 standard error of mean values unless otherwise indicated.
[b] Error statistics with HEC–RAS–predicted velocities were based on differences in the predicted values over the range of n values evaluated for the respective materials.
[c] Represents the overprediction of water surface elevation by HEC–RAS.

Table 2. Mean velocity data from the anemometer and HEC–RAS.

Position from Channel Discharge (m)	Channel Feature	Nominal n Value	Selected Model n Value	Anemometer Mean Velocity (m s^{-1})	Percent Mean Velocity Difference[a]			
					Normal n	High n	Low n	Selected n
0.77	Rock	0.028	0.031	1.18	–11	–3	–13	–3
1.00	Upslope	0.009	0.009	0.75	2	4	3	4
1.23	Weir	0.018	0.018	0.28	–2	–2	–2	–2
1.57	Downslope	0.009	0.009	0.49	11	14	11	11

[a] Percent difference = [(anemometer mean velocity – HEC–RAS mean velocity) / anemometer mean velocity] × 100.

what higher than expected. The differences between the HEC–RAS and measured mean velocities are most likely due to variation in effective Manning n values and to the fact that the classical logarithmic profile and associated boundary layer development in open–channel flow is not well developed in the flume due to the short reach. The shallow depths in the flume caused some problems with achieving the 0.6 depth placement of the probe (the approximate point of mean velocity in a logarithmic profile flow), further contributing to error possibilities. In the rock region, some flow occurred within the rock media, and the shape of the rocks may have caused localized changes in the anemometer mean velocity. The errors represent standard error of the mean of four to five measurements in the two respective channels.

Periphyton (Chlorophyll *a*) Live Biomass

Figure 4 shows the chlorophyll *a* concentration (which characterizes live biomass) at each TSS level by location. The first control run showed a considerably lower chlorophyll *a* concentration than the second control run. In addition, in the first run, the chlorophyll *a* concentration decreased along the flume length, whereas it was more or less uniform in the second run. This may have been due to acclimatization to the flume. Variation is indicated by the error bars for the mean values.

An ANOVA revealed that interactions existed ($P \leq 0.05$) between TSS level and flume position. Data were re–analyzed by location, and the SNK multiple–comparison test was used to determine if differences existed between treatments. Selected SNK results are shown in table 3. The SNK multiple–comparison tests indicated significant ($P \leq 0.05$) differences with chlorophyll *a* at respective locations with TSS level. The markedly low response at the 200 mg L^{-1} level explained the interaction and the significance of location.

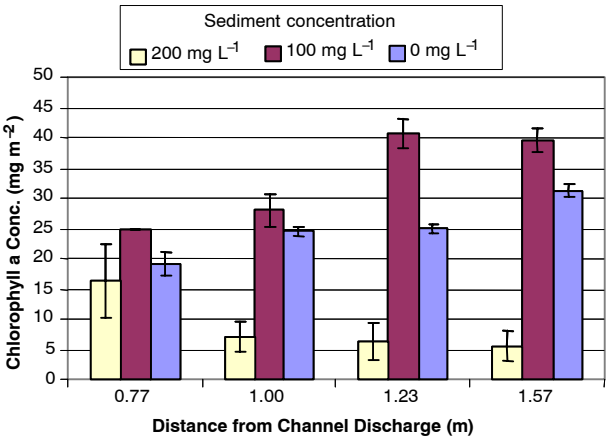

Figure 4. Chlorophyll *a* concentration at each test location as a function of the distance to the channel discharge (downslope = 0.77 m, weir = 1.00 m, upslope = 1.23 m, rocks = 1.57 m) with error bars showing standard error of the means.

Chlorophyll *a* concentration at each TSS level is plotted against mean velocity in figure 5. The control and 100 mg L^{-1} TSS levels showed a decrease in chlorophyll *a* concentration with increasing mean velocity. At the 200 mg L^{-1} TSS level, there was an increase in chlorophyll *a* concentration with increasing mean velocity, suggesting a compensation mechanism by the periphyton to counter the reduced light in the presence of high TSS loadings. The distinguishing feature is the linearity, with a decreasing slope as TSS increases and an adverse slope at the highest TSS. The R^2 values ranged from 0.63 to 0.91; however, the number of points is limited. Increased TSS levels of 100 mg L^{-1} likely induced a growth response. Flow conditions had a variable effect. The TSS level of 200 mg L^{-1} likely resulted in shading to the extent that the

Table 3. Selected Student–Newman–Keuls (SNK) results for the periphyton study.

Response Variable	Factor	Mean Square Error	DF	Factor Value	Mean	Different from Indicated Treatment ($P \leq 0.05$)
Chlorophyll *a* (µg L^{-1})	Sed. conc. (mg L^{-1})	2.695657	118	Sed. Conc. (mg L^{-1})	Chlorophyll (µg L^{-1})	
			44	200	1.005145	0, 100
			44	0	2.34192	200, 100
			44	100	3.208373	200, 0
Pheophytin (µg L^{-1})	Sed. conc. (mg L^{-1})	3.136054	118		Pheophytin (µg L^{-1})	
			44	100	0.4370155	0
			44	200	0.620468	0
			44	0	2.396428	100, 200
Filament length (cm)	Sed. conc. (mg L^{-1})	0.1167625	8		Filament length (cm)	
			6	200	1.405	100, 0
			6	100	4.377	200
			6	0	4.802	200

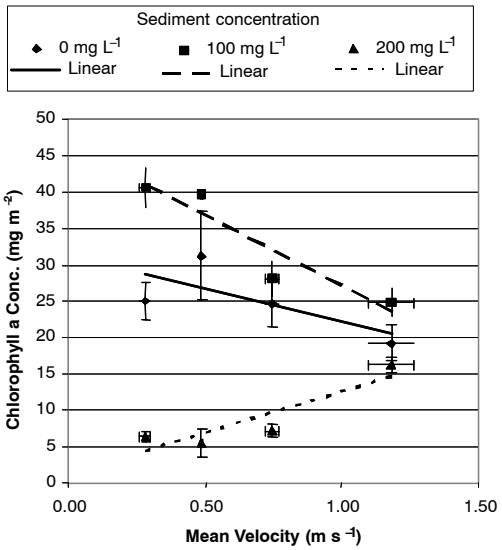

Figure 5. Chlorophyll *a* concentration as a function of mean velocity at each location (downslope = 1.18 m s^{-1}, weir = 0.75 m s^{-1}, upslope = 0.28 m s^{-1}, rocks = 0.49 m s^{-1}) with error bars showing standard error of the means in the *x* and *y* directions.

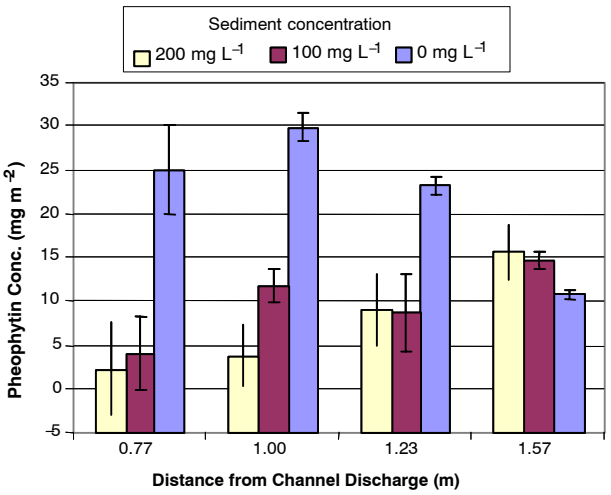

Figure 7. Pheophytin concentration at each location as a function of the distance to the channel discharge (downslope = 0.77 m, weir = 1.00 m, upslope = 1.23 m, rocks = 1.57 m) with error bars showing standard error of the means.

periphyton could not adequately compensate for adverse flow conditions. The highest velocity occurred at the lowest depth; thus, the shading was minimized there, allowing the most growth at the high TSS level.

Similar trends were noted with shear velocity (fig. 6). The measured RMS velocity resulted in a poorer linear fit and thus is not shown. The discrepancy suggests that the isotropic turbulence assumption is questionable. Hondzo and Wang (2002) found periphyton biomass to be lowest in stagnant flow conditions and maximal at a shear velocity of 0.007 m s^{-1}. Our study, which did not include shear velocities less than 0.02 m s^{-1}, was consistent with Hondzo and Wang (2002) with lower turbidities (fig. 6) but not with the 200 mg L^{-1} level. The Hondzo and Wang (2002) study did not consider the TSS variable. The compensation mechanism would likely affect the Hondzo and Wang (2002) results. The RMS velocity trends (not shown) were somewhat similar, except that trends were curvilinear or notably different, particularly as TSS level increased.

Figure 7 shows pheophytin (dead and senesced cell) levels at each TSS level by test region. Pheophytin concentrations decreased with increasing TSS level in the rock and upslope locations. In the weir region, pheophytin was highest in the control and lowest in the 100 mg L^{-1} level. In the downslope location, pheophytin concentration increased with increasing TSS level.

Pheophytin concentration was analyzed with TSS level and flume position to determine significant interactions ($P \leq 0.05$). SNK multiple-comparison tests were run to determine

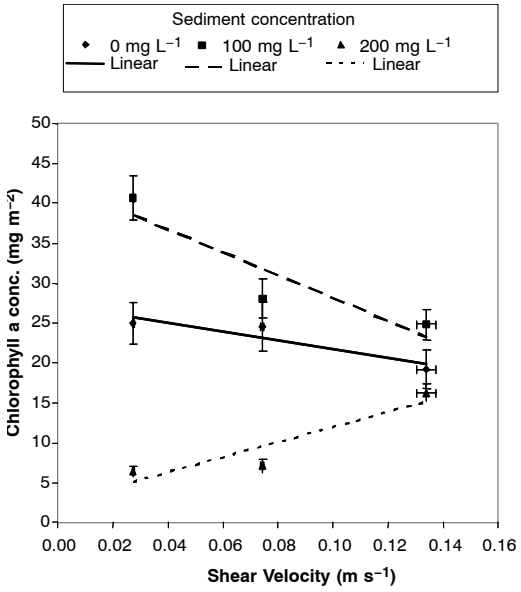

Figure 6. Chlorophyll *a* concentration as a function of shear velocity at each location (downslope = 1.18 m s^{-1}, weir = 0.75 m s^{-1}, upslope = 0.28 m s^{-1}, rocks = 0.49 m s^{-1}) with error bars showing standard error of the means in the *x* and *y* directions.

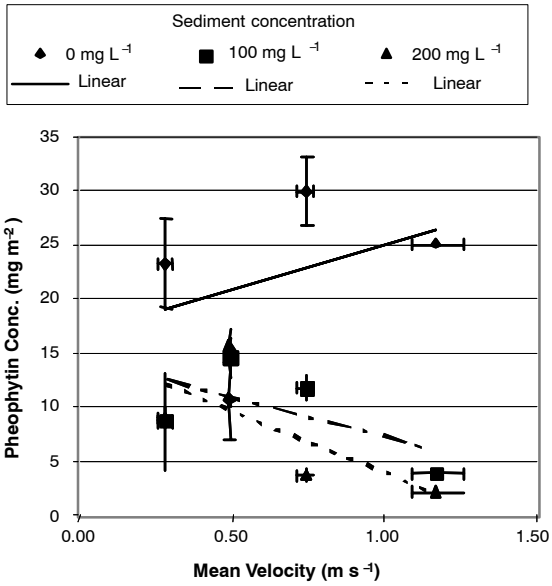

Figure 8. Pheophytin concentration as a function of mean velocity at each location (downslope = 1.18 m s^{-1}, weir = 0.75 m s^{-1}, upslope = 0.28 m s^{-1}, rocks = 0.49 m s^{-1}) with error bars showing standard error of the means in the *x* and *y* directions.

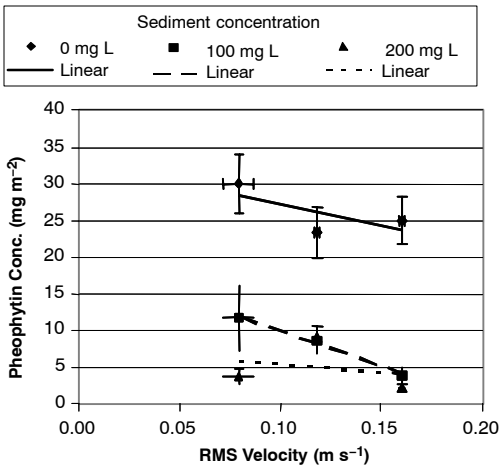

Figure 9. Pheophytin concentration as a function of RMS velocity at each location (downslope = 0.16 m s^{-1}, weir = 0.08 m s^{-1}, upslope = 0.12 m s^{-1}) with error bars showing standard error of the means in the *x* and *y* directions.

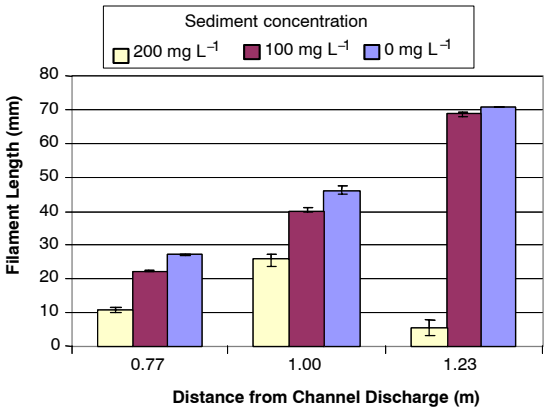

Figure 10. Filament length at each location as a function of the distance to the channel discharge (downslope = 0.77 m, weir = 1.00 m, and upslope = 1.23 m) with error bars showing standard error of the means.

if any TSS level showed a significant difference in the concentration of pheophytin. Pheophytin concentration at the control level was significantly different ($P \leq 0.05$) from the 100 mg L^{-1} and 200 mg L^{-1} levels (table 3). The high TSS results are consistent with the USEPA (2001) upper threshold of 284 mg L^{-1}. Pheophytin concentration at each TSS level was plotted against mean velocity (fig. 8). Pheophytin concentrations varied at each TSS level. Linear fits are shown; however, all the R^2 values were lower than with chlorophyll *a* shown in figure 5.

Pheophytin concentration plotted versus RMS velocity is shown in figure 9. The RMS velocity was more efficacious for plotting pheophytin than was the shear velocity, causing us to question the isotropic turbulence assumption (figs. 2 and 6). Pheophytin tended to decrease with RMS velocity in the range tested for lower TSS levels. At the highest TSS, the upslope (RMS vel. = 0.12 m s^{-1}) value gave the highest pheophytin concentration. The RMS plotting variable appeared to improve the predictions and is worthy of additional testing. The results for pheophytin seem to be consistent with the notion that pheophytin would increase in zones where physical stress was greatest and/or zones where TSS was greatest. The intermediate 100 mg L^{-1} level where presumed compensation was occurring was difficult to interpret.

A question arises concerning the nature of the periphyton-pheophytin response: Are we seeing periphyton (living) transition to pheophytin (dead) due to a physical response or to physiological senescence? Our underlying presupposition is that the pheophytin response was due more to the physical environment than simply to the physiological response that one would expect to observe under standard growth conditions. The physical environment quite likely influences the physiological response. In other words, we feel that the faster velocities and higher TSS levels create conditions in which sustained injury will occur at greater frequency and thus shorten the life of the biological material.

Periphyton Filament Length

Filament length was obtained by averaging six random samples of the filament lengths in each region. Filament length was not measured in the rock section due to the inability to obtain reliable lengths from the rock surfaces. (The tile surface was used specifically to facilitate the biomass measurements). Figure 10 shows filament length at each TSS level for each location. As TSS level increased, mean filament length generally increased, except at the 200 mg L^{-1} level where reduced light availability likely hindered growth.

The filament length evaluation was generally consistent with the biomass evaluation. TSS level and location were significant at the 95% confidence interval, with interactions present. Filament length at the 200 mg L^{-1} TSS was significantly ($P \leq 0.05$) shorter than the filament lengths at the 100 mg L^{-1} and control TSS levels. There was no significant difference ($P \leq 0.05$) between the filament lengths at the control and 100 mg L^{-1} TSS levels. Further analyses revealed that the 200 mg L^{-1} TSS level was responsible for the TSS level interaction. Filament lengths in the lower and upper locations were significant ($P \leq 0.05$) based on results of analyses at the control and 100 mg L^{-1} TSS levels.

Filament length versus mean velocity is plotted in figure 11. Filament length decreased with increasing mean velocity at the control and 100 mg L^{-1} TSS levels. This is consistent with the increased physical stress at higher mean velocities. Filament length was linear with mean velocity at the control and 100 mg L^{-1} TSS levels, with R^2 values above 0.95. At the 200 mg L^{-1} TSS level, little or no correlation existed between filament length and mean velocity, which is

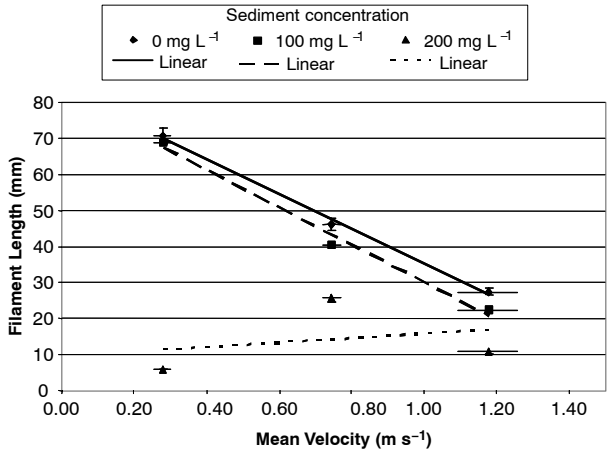

Figure 11. Filament length as a function of mean velocity at each location (upslope = 0.28, weir = 0.75, downslope = 1.18) with error bars showing standard error of the means in the *x* and *y* directions.

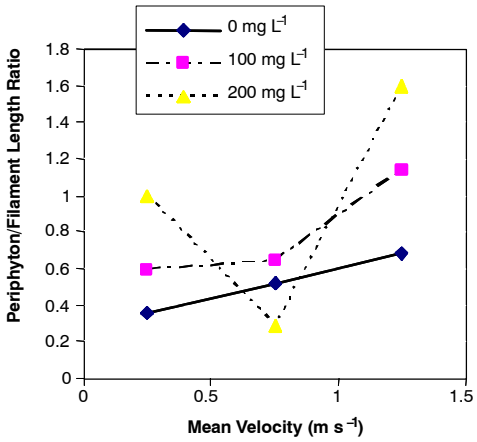

Figure 12. Ratio of periphyton to filament length versus mean velocity by TSS level.

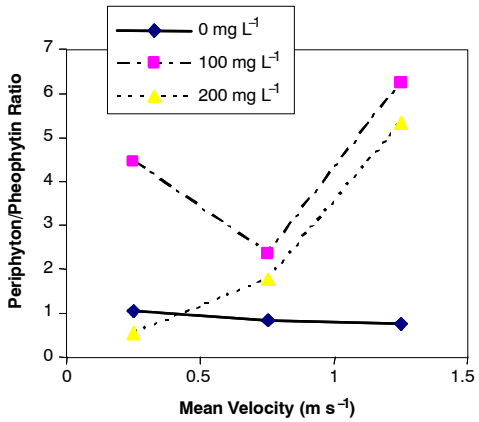

Figure 13. Ratio of periphyton to pheophytin versus mean velocity by TSS level.

consistent with the notion that TSS-induced shading dominated. TSS-induced shading would be greatest in the lower velocities, since depth was greater in those cases. Plotting filament length versus RMS velocity and other variables added little additional information.

Filament orientation was observed to vary by test region. In the upper testing area (lower velocities), the filaments were erect, while in the lower location, higher velocities forced the periphyton to a prostrate orientation. TSS addition also appeared to affect growth habits. In the upper location, the presence of 200 mg L^{-1} TSS caused the periphyton to grow in thin mats that made length measurements difficult. In the middle location (weir), the periphyton filaments trapped a visible amount of kaolin in them, so the filaments could be seen protruding from a thin sediment layer. The lower location generally showed little apparent differences with TSS, except that higher TSS slowed development.

In the higher TSS runs, growth patterns varied farther downstream from the weir. The tiles adjacent to the weir evidenced a coarser filament texture than found farther below the weir. With no TSS, the periphyton grew in filaments that required significant effort for biomass removal from the test tiles. As the kaolin was introduced, the periphyton shifted to easily removed thin mats. The periphyton in the upper location was more easily removed than periphyton from the other locations. The periphyton in the upper (rocks) region with low velocity grew in thicker quantities, while the lower discharge region grew more sparsely at first. Persistent high velocities and low TSS seemed to favor the most tenacious attachment. Increases in TSS reduced attachment tenacity in high-velocity regions and tended to decrease growth in all regions.

Periphyton biomass was lower than that reported by Hondzo and Wang (2002), likely due to lower light levels (and TSS) in this study. Filament length decreased as shear velocity increased at the control and 100 mg L^{-1} TSS levels. At the 200 mg L^{-1} TSS level, the filament length increased and then decreased as shear velocity increased. Filament length may be more sensitive to the 200 mg L^{-1} TSS level than to shear velocity. Ratios of periphyton biomass to filament length and periphyton to pheophytin biomass were plotted versus mean velocity and TSS (figs. 12 and 13).

The periphyton/filament length ratio tended to be lowest at velocities less than 0.75 m s^{-1} except in the high TSS case, where both periphyton and filament length were low. Low velocities and low to moderate TSS would provide the most biomass with longest filament length for grazing organisms and nutrient filtering. High periphyton/pheophytin ratios were associated with high TSS, velocities exceeding ~0.5 m s^{-1}, or both. Velocity values exceeding ~0.5 m s^{-1} may result in periphyton having shorter and dense filaments at low TSS levels. These results suggest that, for maximum periphyton development, velocity should not exceed ~0.5 m s^{-1} and TSS should not exceed moderate (e.g., 100 mg L^{-1}) levels to maximize benefits of nutrient removal (e.g., Vyzamal, 1988; Adey et al., 1993; Dodds, 2003). The 0.5 m s^{-1} threshold is near that used for incipient sediment transport in sewer design and in sediment transport studies. From a system management perspective, a cyclical (e.g., with a period of two weeks or more) velocity change above or below a 0.5 m s^{-1} threshold may allow a dense periphyton cover to develop, which would be sloughed, potentially causing debris problems at a downstream point. The mean velocity threshold of 0.5 m s^{-1} may be replaced by a friction velocity threshold of 0.05 m s^{-1} or an RMS velocity threshold of 0.1 m s^{-1} in other hydraulic configurations; however, further work is needed to evaluate flows through various meshes or devices other than the channel and weir evaluated herein.

The recirculation flume as a microcosm for simulating field channel conditions could be readily extended to include various chemical toxicity factors by specifying appropriate materials for all water-contacting surfaces. Additional experiments including additional TSS levels, additional turbulence studies, and experiments in which nutrient and toxicity interactions are evaluated would further clarify the implications of periphyton management on systems engineered around a channel conveyance.

Conclusions

The recirculation flume appears to be a useful microcosm for periphyton studies based on this and other cited work. The recirculation flume (with occasional water replacement) makes extending the studies to include various chemical effects feasible. HEC-RAS modeled the one-dimensional velocities within 11%, after varying the roughness values within published extremes, and somewhat overpredicted surface water elevation. The overprediction was attributed to

published errors in the HEC-RAS model and to the fact that the shortness of the flume aggravated difficulties with properly simulating inlet conditions. It is concluded that a recirculating flume coupled with HEC-RAS can be used to roughly, but not precisely, approximate selected hydraulic and physical factors affecting periphyton growth in a field channel.

Significant interactions between biological response and hydraulic and TSS factors were observed, and the study suggested several indicators of periphyton-pheophytin response that are potentially relevant to channel-based systems. Mean velocity appears to be a good indicator of periphyton biomass, as indicated by chlorophyll *a* and filament length at the TSS levels evaluated. Periphyton results plotted with shear velocity generally confirmed a major study (Hondzo and Wang, 2002) at zero TSS. Additional turbulence measurements beyond shear velocity did not shed much additional light on the periphyton or pheophytin response.

Pheophytin tended to be highest in conditions having lower chlorophyll *a* values, consistent with the notion that regimes with physical stress limiting chlorophyll *a* production would have the highest dead biomass. The inclusion of pheophytin evaluations in a periphyton study is complimentary in that it appears to provide an indication of stress levels.

High TSS generally hindered growth, likely due to deposition and TSS reducing available light. An apparent growth compensation effect was observed at the intermediate TSS level. In this study, the periphyton/filament length ratio tended to be lowest at velocities less than ~0.5 m s^{-1} except in the high TSS case, where both periphyton and filament length were low. Low velocities and low to moderate TSS would provide the most biomass for grazing organisms. High periphyton/pheophytin ratios were associated with high TSS, velocities exceeding 0.5 m s^{-1}, or both. Sloughing could occur in systems with a pulsing velocity where the pulse period was long enough for growth to occur in the quiescent interval, which may have other effects downstream.

Acknowledgements

Thanks to Drs. Amy Rosemond, Alan Covich, William Kisaalita, and Mark Eiteman for sharing their knowledge, experience, and key facilities. Ryan Adolfson, Javier Sayago, and Antonio Travassos provided technical help. Funding for this project was provided by the Georgia Agricultural Experiment Station.

References

Adey, W., C. Luckett, and K. Jensen. 1993. Phosphorus removal from natural waters using controlled algal production. *Restor. Ecol.* 1(1): 29-39.

Asaeda, T., and D. Hong Son. 2000. Spatial structure and populations of a periphyton community: A model and verification. *Ecological Modelling* 133(3): 195-207.

Bergstedt, M. S., M. M. Hondzo, and J. B. Cotner. 2004. Effects of small-scale fluid motion on bacterial growth and respiration. *Freshwater Biol.* 49(1): 28-40.

Birkett, C. 2005. The effect of flow regime and turbidity on periphyton in a laboratory system. MS thesis. Athens, Ga.: University of Georgia, Department of Biological and Agricultural Engineering.

Bockelmann, B. N., E. K. Fenrich, B. Lin, and R. A. Falconer. 2004. Development of an ecohydraulics model for stream and river restoration. *Ecological Eng.* 22(4-5): 227-235.

Bokn, T. L., F. E. Moy, H. Christie, R. Karez, K. Kersting, P. Kraufvelin, C. Lindblad, N. Marba, M. F. Pedersen, and K. Sorensen. 2002. Are rocky shore ecosystems affected by nutrient enriched seawater? Some preliminary results from a mesocosm experiment. *Hydrobiologia* 484: 167-175.

Boynton, W. R., D. Baird, and R. E. Ulanowicz. 1995. Seasonal nitrogen dynamics in Chesapeake Bay: A network approach. *Estuarine, Coastal, and Shelf Science* 41(2): 137-162.

Brunner, G. W. 2002. HEC-RAS river analyses system: Hydraulic reference manual. Davis, Cal.: U.S. Army Corps of Engineers, Hydrologic Engineering Center.

Chow, V. T. 1959, *Open-Channel Hydraulics.* New York, N.Y.: McGraw-Hill.

Cokgor, S., and S. Kucukali. 2004. Oxygen transfer in flow around and over stones placed in a laboratory flume. *Ecological Eng.* 23(3): 205-219.

Dodds, W. K. 2003. The role of periphyton in phosphorus retention in shallow freshwater aquatic systems. *J. Phycol.* 39(5): 840-849.

Eriksson, P. G., and S. E. B. Weisner. 1996. Functional differences in epiphytic microbial communities in nutrient-rich freshwater ecosystems: An assay of denitrifying capacity. *Freshwater Biol.* 36(3): 555-562.

Guillard, R. R., and C. J. Lorenzen. 1972. Yellow-green algae with chlorophyllide *c*. *J. Phycol.* 8(1): 10-14.

Harding, J. S., R. G. Young, J. W. Hayes, K. A. Shearer, and J. D. Stark. 1999. Changes in agricultural intensity and river health along a river continuum. *Freshwater Biol.* 42(2): 345-357.

Hill, B. H., A. T. Herlihy, P. R. Kaufmann, S. J. DeCelles, and M. A. Vander Borgh. 2003. Assessment of streams of the eastern United States using a periphyton index of biotic integrity. *Ecological Indicators* 2(4): 325-338.

Hill, W. R. 1996. Factors affecting benthic algae. In *Algal Ecology: Freshwater Benthic Ecosystems*, 341-374. R. J. Stevenson, M. L. Bothwell, and R. L. Lowe, eds. San Diego, Cal.: Academic Press.

Hintze, J. L. 2004. *Number Cruncher Statistical System.* 2004 version. Kaysville, Utah: NCSS.

Hondzo, M., and H. Wang. 2002. Effects of turbulence on growth and metabolism of periphyton in a laboratory flume. *Water Resources Res.* 38(12): 1277.

Lau, Y. L., and D. Liu. 1993. Effect of flow rate on biofilm accumulation in open channels. *Water Res.* 27(3): 355-360.

Mattila, J., and R. Raisanen. 1998. Periphyton growth as an indicator of eutrophication: An experimental approach. *Hydrobiologia* 377: 15-24.

Nezu, I., A. Kadota, and H. Nakagawa. 1997. Turbulent structure in unsteady depth-varying open-channel flows. *J. Hydraulic Eng.* 123(9): 752-763.

Nikora, V. I., D. G. Goring, and B. J. F. Biggs. 1997. On stream periphyton-turbulence interactions. *New Zealand J. Marine and Freshwater Res.* 31(4): 435-448.

Nikora, V. I., D. G. Goring, and B. J. F. Biggs. 2002. Some observations of the effects of micro-organisms growing on the bed of an open channel on the turbulence properties. *J. Fluid Mech.* 450: 317-341.

Parkhill, K. L., and J. S. Gulliver. 2002. Effect of inorganic sediment on whole-stream productivity. *Hydrobiologia* 472: 5-17.

Pringle, C. M., and T. Yamasaki. 1997. Effects of fishes on algal response to storms in a tropical stream. *Ecology* 78(8): 2432-2442.

Quinn, J. M., C. W. Hickey, and W. Linklater. 1996. Hydraulic influences on periphyton and benthic macroinvertebrates: Simulating the effects of upstream bed roughness. *Freshwater Biol.* 35(2): 301-309.

Riegman, R., J. D. L. Van Bleuswuk, and C. P. D. Brussard. 2002. The use of dissolved esterase activity as a tracer of phytoplankton lysis. *Limnol. Oceanogr.* 47(3): 916-920.

Rosemond, A. D. 1993. Interactions among irradiance, nutrients, and herbivores constrain a stream algal community. *Oecologia* 94(4): 585-594.

Rosemond, A. D., P. J. Mulholland, and J. W. Elwood. 1993. Top-down and bottom-up control of stream periphyton: Effects of nutrients and herbivores. *Ecology* 74(4): 1264-1280.

Rosemond, A. D., H. S. Weyers, M. J. Paul, J. L. Greenwood, and D. S. Leigh. 2001. Benthic algal biomass in the Etowah basin and implications to establishing nutrient criteria in streams. In *Proc. 2001 Georgia Water Resources Conf.* K. J. Hatcher, ed. Athens, Ga.: The University of Georgia, Institute of Ecology.

Sabater, S., J. Armengol, E. Comas, F. Sabater, I. Urrizalqui, and I. Urrutia. 2000. Algal biomass in a disturbed Atlantic River: Water quality relationships and environmental implications. *Science Total Environ.* 263(1-3): 185-195.

Sansone, U., M. Belli, M. Riccardi, A. Alonzi, Z. Jeran, J. Radojko, B. Smodis, M. Montanari, and F. Cavolo. 1998. Adhesion of water-borne particulates on freshwater biota. *Science Total Environ*. 219(1): 21-28.

Saravia, L. A., F. Momo, and L. D. Boffi Lissin. 1998. Modelling periphyton dynamics in running water. *Ecological Modelling* 114(1): 35-47.

Schofield, K. A., C. M. Pringle, and J. L. Meyer. 2004. Effects of increased bed load on algal and detrital-based stream food webs: Experimental manipulation of sediment and macroconsumers. *Limnol. Oceanogr.* 49(4): 900-909.

Simons, D. B., and F. Senturk. 1992. *Sediment Transport Technology: Water and Sediment Dynamics*. Littleton, Colo.: Water Resources Publications.

Steinman, A. D., and G. A. Lamberti. 1996. Biomass and pigments of benthic algae. In *Methods in Stream Ecology*, 295-309. F. R. Hauer, and G. A. Lamberti, eds. San Diego, Cal.: Academic Press.

Stevenson, R. J. 1996. The stimulation and drag of current. In *Algal Ecology: Freshwater Benthic Ecosystems*, 341-374. R. J. Stevenson, M. L. Bothwell, and R. L. Lowe, eds. San Diego, Cal.: Academic Press.

Tollner, E. W., T. C. Rasmussen, B. Upchurch, and J. Sikes. 2005. Simulated moving bed form effects on real-time in-stream sediment concentration measurement with densitometry. *J. Hydraulic Eng. ASCE* 131(12): 1141-1144.

USEPA. 2001. United Chattooga River watershed ecological/sedimentation project. Federal Interagency Sedimentation Conference. Washington, D.C.: U.S. Environmental Protection Agency.

Vyzamal, J. 1988. The use of periphyton communities for nutrient removal from polluted streams. Hydrobiologia 166(3): 225-237.